

The Infra-Red Spectrum and Molecular Constants of C¹²O¹⁶ and C¹³O¹⁶

ROBERT T. LAGEMANN,* ALVIN H. NIELSEN,** AND FRED P. DICKEY***

The Ohio State University, Columbus, Ohio

(Received May 5, 1947)

The infra-red spectrum of carbon monoxide has been investigated with a 7200 line-per-inch grating. The fundamental bands of C¹²O¹⁶ and C¹³O¹⁶ and the overtone of C¹²O¹⁶ were measured. The rotational structure has been analyzed by means of combination relations, and the following new values of the molecular constants have been obtained: $\omega_e = 2169.60 \text{ cm}^{-1}$, $\omega_e' = 2121.33 \text{ cm}^{-1}$, $x_e\omega_e = 13.22 \text{ cm}^{-1}$, $(x_e\omega_e)' = 12.64 \text{ cm}^{-1}$, $B_e = 1.9238 \text{ cm}^{-1}$, $B_e' = 1.8465 \text{ cm}^{-1}$, $\alpha = 0.0175 \text{ cm}^{-1}$, $\alpha' = 0.0169 \text{ cm}^{-1}$, $I_e = 14.548 \times 10^{-40} \text{ g cm}^2$, $I_e' = 15.157 \times 10^{-40} \text{ g cm}^2$, r_e (average for both molecules) = $1.1291 \times 10^{-8} \text{ cm}$. The primed constants refer to the isotopic molecule.

1. INTRODUCTION

THE infra-red spectrum of carbon monoxide has been examined by a number of investigators,¹ using spectrometers with various amounts of resolving power. The most complete of these investigations was that of Whitcomb and Lagemann who used 3600 and 4800 line-per-inch gratings to resolve the rotational structure of the fundamental and overtone bands of C¹²O¹⁶.

TABLE I. The rotation lines in the fundamental band of C¹²O¹⁶.

Iden- tifica- tion	Positive (R) branch (cm ⁻¹)			Negative (P) branch (cm ⁻¹)			
	ν Obs.	ν Calc.	Differ- ence	Iden- tifica- tion	ν Obs.	ν Calc.	Differ- ence
R(0)	2147.05	2146.94	+0.11	P(1)	2139.32	2139.33	-0.01
R(1)	2150.83	2150.70	+0.13	P(2)	2135.48	2135.46	+0.02
R(2)	2154.44	2154.44	0.00	P(3)	2131.49	2131.56	-0.07
R(3)	2158.13	2158.13	0.00	P(4)	2127.61	2127.63	-0.02
R(4)	2161.83	2161.79	+0.04	P(5)	2123.62	2123.66	-0.04
R(5)	2165.44	2165.41	+0.03	P(6)	2119.64	2119.65	-0.01
R(6)	2169.05	2168.99	+0.06	P(7)	2115.56	2115.61	-0.05
R(7)	2172.63	2172.54	+0.09	P(8)	2111.48	2111.54	-0.06
R(8)	2176.12	2176.06	+0.06	P(9)	2107.33	2107.43	-0.10
R(9)	2179.57	2179.53	+0.04	P(10)	2103.12	2103.28	-0.16
R(10)	2183.14	2182.98	+0.16	P(11)	2099.01	2099.10	-0.09
R(11)	2186.47	2186.39	+0.08	P(12)	2094.69	2094.89	-0.20
R(12)	2189.84	2189.77	+0.07	P(13)	2090.56	2090.64	-0.08
R(13)	2193.19	2193.11	+0.08	P(14)	2086.27	2086.35	-0.08
R(14)	2196.53	2196.41	+0.12	P(15)	2081.95	2082.03	-0.08
R(15)	2199.77	2199.68	+0.09	P(16)	2077.57	2077.68	-0.11
R(16)	2202.96	2202.92	+0.04	P(17)	2073.19	2073.29	-0.10
R(17)	2206.19	2206.12	+0.07	P(18)	2068.69	2068.86	-0.17
R(18)	2209.31	2209.28	+0.03	P(19)	2064.31	2064.40	-0.09
R(19)	2212.46	2212.41	+0.05	P(20)	2059.79	2059.91	-0.12
R(20)	2215.66	2215.51	+0.15	P(21)	2055.31	2055.38	-0.07
R(21)	2218.67	2218.57	+0.10	P(22)	2050.72	2050.81	-0.09
R(22)	2221.56	2221.59	-0.03	P(23)	2046.14	2046.21	-0.07
R(23)	2224.63	2224.58	+0.05				
R(24)	2227.55	2227.54	+0.01				
R(25)	2230.49	2230.46	+0.03				
R(26)	2233.34	2233.34	0.00				
R(27)	2236.06	2236.19	-0.13				
R(28)	2238.89	2239.01	-0.12				

* Emory University, Emory University, Georgia.

** The University of Tennessee, Knoxville, Tennessee.

*** The Ohio State University, Columbus, Ohio.

¹ E. F. Lowry, J. Optical Soc. Am. **8**, 647 (1924); C. P. Snow and E. K. Rideal, Proc. Roy. Soc. **A125**, 462 (1929); S. E. Whitcomb and R. T. Lagemann, Phys. Rev. **55**, 181 (1939).

More recently, Lagemann,² using the same spectrometer, observed the fine structure of the C¹³O¹⁶ fundamental band superposed on the fundamental band of C¹²O¹⁶.

The present paper is the result of an attempt to observe the complete spectrum of both C¹²O¹⁶ and C¹³O¹⁶ and to compute new values for the constants from these data. The bands observed were the fundamental and overtone of C¹²O¹⁶, and the fundamental of C¹³O¹⁶. The overtone of the isotopic molecule, though detected, could not be measured with the gas samples available. A sample of gas enriched with C¹³O¹⁶ is being obtained, and the overtone will be reported in a future note. Several of the stronger lines of this band were, however, observed, and their position agreed with line positions predicted from the constants given in Table IV.

2. EXPERIMENTAL

Two absorption cells fitted with rocksalt windows containing pure carbon monoxide were used in observing these bands: one was 8 cm long and filled to a pressure of 12 cm of mercury, and the other was 20 cm long and filled to atmospheric pressure. The 8-cm cell was found to be of the proper length for the fundamentals, while the 20-cm cell was required to observe the overtone.

The same spectrometer as was used by Whitcomb and Lagemann was equipped with a 7200 line-per-inch replica grating and used for these measurements. Mercury lines in several orders were used to calibrate the instrument. All line positions and frequencies have been reduced to

² R. T. Lagemann, J. Chem. Phys. **10**, 193 (1942).

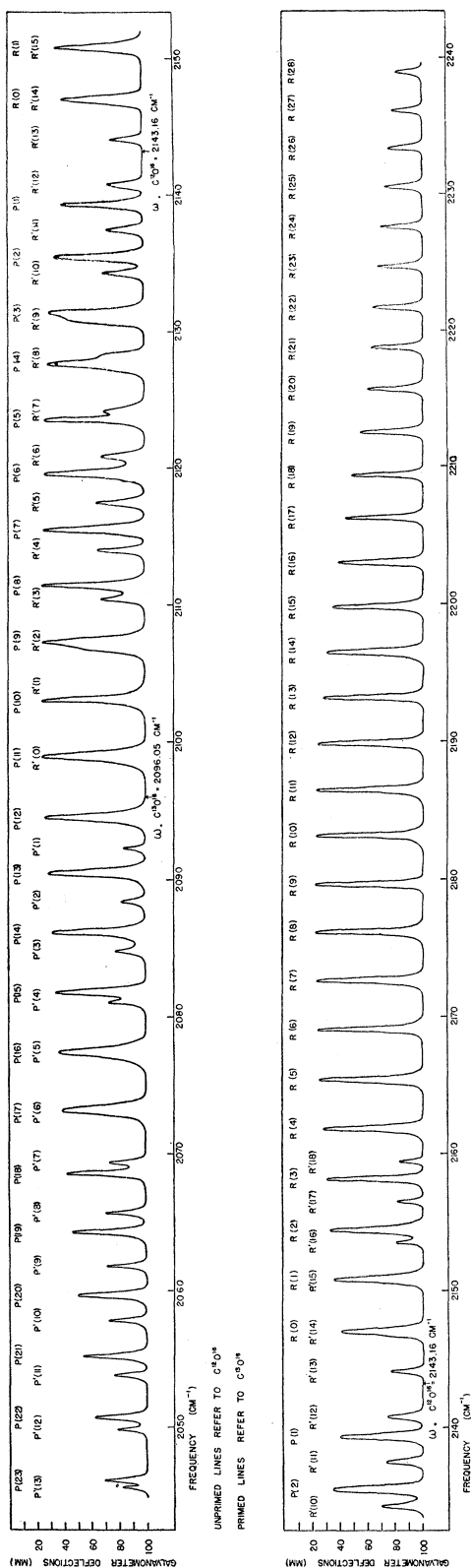


Fig. 1. Fundamental vibration-rotation band of C¹²O¹⁶ and C¹³O¹⁶.

vacuum. A vacuum thermocouple was used as a radiation detector. The thermocouple output voltage was amplified by a Moll relay and finally observed as deflections of a Leeds and Northrup high sensitivity galvanometer. Angular positions of the grating were recorded and converted to frequencies by the usual relation $\nu(\text{cm}^{-1}) = K \nu \csc \theta$ where $K \nu$ is the instrument constant. Observations were made at spectral intervals of about 0.07 cm^{-1} , and the slits of the spectrometer were set to include a spectral interval of about 0.25 cm^{-1} . It is believed that the line positions are, in general, reliable to about $\pm 0.07 \text{ cm}^{-1}$.

3. FUNDAMENTAL BANDS

In Fig. 1 is shown a somewhat idealized curve representing the galvanometer deflections in cm as ordinates plotted *versus* frequencies in cm^{-1} as abscissae for the fundamental bands. Several complete sets of observations were made over the whole region, and only those lines appearing in all sets of observations have been represented in the figure. This has the effect of eliminating from the final curve the thermal agitation errors. In this figure a decrease in galvanometer deflections indicates increased absorption of the incident radiation by the gas. The unprimed lines in Fig. 1 are due to C¹²O¹⁶ and are much more intense than the primed lines which are due to C¹³O¹⁶.

The double space at the band center caused by the missing line, a characteristic of infra-red spectra of diatomic molecules, was less easily identified for C¹³O¹⁶ than for C¹²O¹⁶ because some of the isotopic lines were obscured by the much more intense C¹²O¹⁶ lines. It was, therefore, not difficult to assign the rotational quantum number, J , to the levels, in the case of C¹²O¹⁶. After a little study the isotopic lines were also identified without ambiguity. Tables I and II list the frequencies of the lines in cm^{-1} for both molecules. The appropriate J values for the initial levels are given in adjacent columns. Frequencies computed from Eq. (4) and the constants in Table IV are also listed. The agreement between observed and computed values is within the experimental error in most cases.

4. OVERTONE BAND

In Fig. 2 is shown the curve for the overtone band of C¹²O¹⁶ plotted in galvanometer deflec-

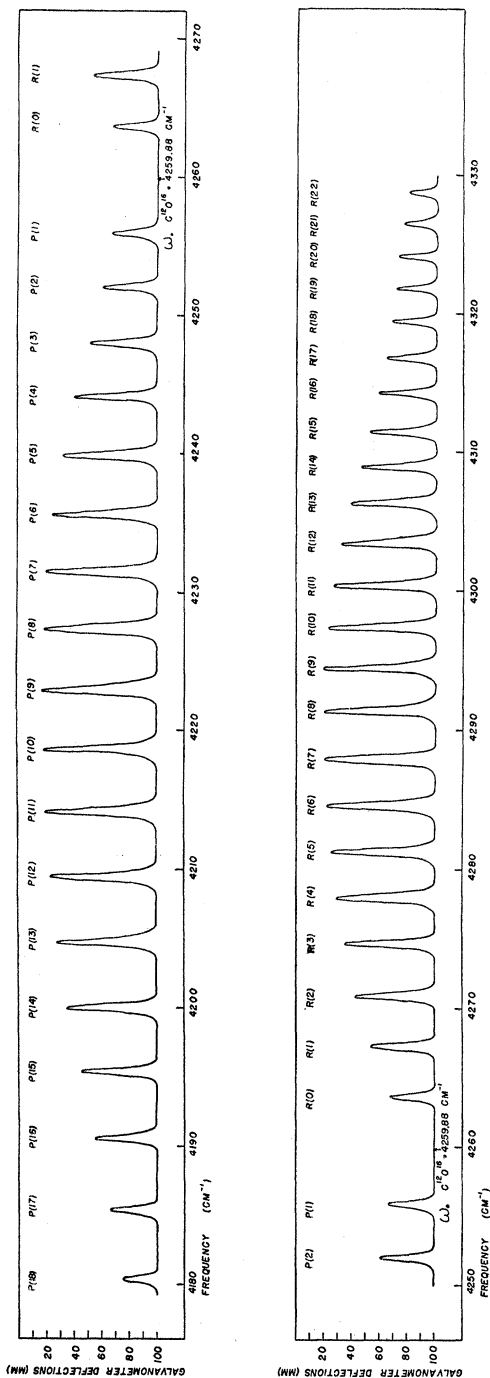


FIG. 2. First overtone vibration-rotation band of $C^{16}O^{16}$.

tions *versus* frequencies in cm^{-1} . Several lines of the overtone of the isotopic molecule were observed, but not enough to enable an analysis to be made. The positions of these lines, though not absolutely identified, agreed with line positions predicted by using Eq. (4) and the constants found in Table IV. Table III lists the observed and computed line positions for the normal molecule with the appropriate J value for the initial level in an adjacent column.

5. ANALYSIS OF THE BANDS

The energy of an oscillating rotator in quantum mechanics is given by the expression:

$$E_{v,J}/hc = \omega_e(v + \frac{1}{2}) - x_e\omega_e(v + \frac{1}{2})^2 + \dots + B_v J(J+1) - D_v J^2(J+1)^2 + \dots, \quad (1)$$

where $E_{v,J}/hc$ = energy in cm^{-1} , v = vibration quantum number, J = rotation quantum number, ω_e = vibrational frequency for infinitesimal amplitude (cm^{-1}), i.e., $v=0, J=0$, $x_e\omega_e$ = the anharmonic term in the vibration (cm^{-1}), $B_v = B_e - \alpha(v + \frac{1}{2})$, the principal rotation term (cm^{-1}), $B_e = h/8\pi^2 c I_e$ (cm^{-1}), α = a constant measuring the dependence of B_v on the vibration (cm^{-1}), D_v = a rotational term related to the centrifugal stretching of the molecule (cm^{-1}). D_v may be neglected in the present case.

The band center, or position of the "missing line" of the fundamental and first overtone $\nu(v=0-1)$ and $\nu(v=0-2)$ in diatomic spectra may be obtained by considering the transitions $v=0$ to $v=1$, and $v=0$ to $v=2$ in Eq. (1) for the non-rotating molecule $J=0$. These frequencies are given by

$$\nu(0-1) = \omega_e - 2x_e\omega_e, \quad (2)$$

$$\nu(0-2) = 2(\omega_e - 3x_e\omega_e). \quad (3)$$

With Eqs. (2) and (3) and the experimentally determined band centers, ω_e and $x_e\omega_e$ may be determined directly. The values are found in Table IV.

The lines of the P and R branches in a vibration-rotation band (i.e., the lines on the low and high frequency sides of the band center) are obtained by considering the $\Delta J = -1$ and $\Delta J = +1$ transitions in Eq. (1). The equation giving the position of these lines is

$$R(m-1) \left. \begin{array}{l} P(m) \\ \end{array} \right\} = \nu \mp m(B' + B'') + m^2(B' - B''), \quad (4)$$

where ν is the frequency of the band center, B'' and B' are the B values in the initial and final states, and where $m=1, 2, 3, \dots$, is the ordinal number of the line. The number in parenthesis $P(m)$ and $R(m-1)$ in Eq. (4) is the J value of the initial rotational state for a line of ordinal number m . For the fundamental $\nu=\nu(0-1)$, $B''=B(v=0)=B_e-\alpha/2$, and $B'=B(v=1)=B_e-3\alpha/2$. For the first overtone $\nu=\nu(0-2)$, $B''=B(v=0)=B_e-\alpha/2$, and $B'=B(v=2)=B_e-5\alpha/2$.

The expressions represented by (4) may be combined to give relations which yield the constants ν , B'' , and B' . These informative equations are:

$$\frac{1}{2}[R(m-1)+P(m)]=\nu+(B'-B'')m^2, \quad (5)$$

$$\frac{1}{2}[R(m-1)-P(m+1)]=(2m+1)B'', \quad (6)$$

$$\frac{1}{2}[R(m)-P(m)]= (2m+1)B'. \quad (7)$$

Equation (5) when plotted with $\frac{1}{2}[R(m-1)+P(m)]$ in cm^{-1} as ordinates versus m^2 as abscissae gives a straight line. The ordinate intercept of this line is ν , the band center, and the slope is $B'-B''$. From a consideration of the B values it may be seen that $[B'(v=1)-B''(v=0)]=-\alpha$. Graphs of Eqs. (6) and (7) when plotted with $\frac{1}{2}[R(m-1)-P(m+1)]$ and $\frac{1}{2}[R(m)-P(m)]$ in cm^{-1} as ordinates versus $(2m+1)$ as abscissae are straight lines, the slopes of which are respectively B'' and B' . In Fig. 3 is shown the graph of $[R(m-1)-P(m+1)]$ versus $2(2m+1)$ from which $B''(v=0)$ for C¹²O¹⁶ was determined. The data from both fundamental and overtone bands were plotted on the same curve to show that the points fit very accurately the relation (6). The curves for relations (5) and (7) are not shown.

6. THEORETICAL

The kinetic and potential energy for the diatomic molecule may be written as

$$T = \frac{1}{2}\mu\dot{Q}'^2, \\ V = \frac{1}{2}KQ'^2 + hcK_{111}Q'^3 + hcK_{1111}Q'^4 + \dots, \quad (8)$$

where Q' represents the displacement coordinate and μ the reduced mass, $m_1m_2/(m_1+m_2)$. It is convenient to introduce the dimensionless coordinate $q = (\mu^2\lambda/\hbar^2)^{1/2}Q'$, where $\lambda = 4\pi^2c^2\omega_e^2$. This leads to the quantum-mechanical relation for T and V given in (9) and (10).

TABLE II. The rotation lines in the fundamental band of C¹³O¹⁶.

Positive (R) branch (cm ⁻¹)				Negative (P) branch (cm ⁻¹)			
Identification	ν Obs.	ν Calc.	Difference	Identification	ν Obs.	ν Calc.	Difference
R(0)	*	2099.69		P(1)	2092.35	2092.37	-0.02
R(1)	*	2103.30		P(2)	2088.57	2088.67	-0.10
R(2)	*	2106.87		P(3)	2084.85	2084.92	-0.07
R(3)	2110.44	2110.41	+0.03	P(4)	2081.12	2081.14	-0.02
R(4)	2113.98	2113.92	+0.06	P(5)	*	2077.33	
R(5)	2117.46	2117.39	+0.07	P(6)	*	2073.49	
R(6)	2120.92	2120.83	+0.09	P(7)	2069.52	2069.61	-0.09
R(7)	2124.20	2124.24	-0.04	P(8)	2065.73	2065.70	+0.03
R(8)	*	2127.61		P(9)	2061.81	2061.75	+0.06
R(9)	*	2130.94		P(10)	2057.81	2057.77	+0.04
R(10)	2134.30	2134.25	+0.05	P(11)	2053.79	2053.76	+0.03
R(11)	2137.49	2137.52	-0.03	P(12)	2049.75	2049.71	+0.04
R(12)	2140.83	2140.95	-0.12	P(13)	2045.61	2045.63	-0.02
R(13)	2144.03	2143.95	+0.08				
R(14)	*	2147.12					
R(15)	*	2150.26					
R(16)	2153.43	2153.36	+0.07				
R(17)	2156.50	2156.42	+0.08				
R(18)	2159.43	2159.46	-0.03				

* These lines were obscured by the C¹²O¹⁶ lines and were not observed.

$$T = -(hc\omega_e/2)(\partial^2/\partial q^2), \quad (9)$$

$$V = hc[(\omega_e/2)q^2 + k_{111}q^3 + k_{1111}q^4 + \dots], \quad (10)$$

where

$$k_{111} = K_{111}(\hbar^2/16\pi^4c^2\mu^2\omega_e^2)^{3/2}, \quad (11)$$

and

$$k_{1111} = K_{1111}(\hbar^2/16\pi^4c^2\mu^2\omega_e^2)^2.$$

In considering the isotopic molecule it is reasonable to assume that the potential energy constants K , K_{111} , K_{1111} are the same as in the normal molecule, but as the reduced mass is different, the frequencies are different. It is possible to verify this assumption for the CO molecule since it leads to the following relations

TABLE III. The rotation lines in the overtone band of C¹²O¹⁶.

Positive (R) branch (cm ⁻¹)				Negative (P) branch (cm ⁻¹)			
Identification	ν Obs.	ν Calc.	Difference	Identification	ν Obs.	ν Calc.	Difference
R(0)	4263.66	4263.64	+0.02	P(1)	4255.95	4256.05	-0.10
R(1)	4267.36	4267.33	+0.03	P(2)	4252.05	4252.15	-0.10
R(2)	4270.84	4270.95	-0.11	P(3)	4248.11	4248.18	-0.07
R(3)	4274.63	4274.50	+0.13	P(4)	4244.12	4244.14	-0.02
R(4)	4277.93	4277.99	-0.06	P(5)	4239.90	4240.03	-0.13
R(5)	4281.31	4281.40	-0.09	P(6)	4235.74	4235.86	-0.12
R(6)	4284.59	4284.74	-0.15	P(7)	4231.57	4231.61	-0.04
R(7)	4287.98	4288.01	-0.03	P(8)	4227.39	4227.29	+0.10
R(8)	4291.39	4291.22	+0.17	P(9)	4223.00	4222.90	+0.10
R(9)	4294.45	4294.35	+0.10	P(10)	4218.57	4218.45	+0.12
R(10)	4297.40	4297.42	-0.02	P(11)	4214.05	4213.92	+0.13
R(11)	4300.47	4300.41	+0.06	P(12)	4209.47	4209.33	+0.14
R(12)	4303.47	4303.34	+0.13	P(13)	4204.75	4204.66	+0.09
R(13)	4306.34	4306.19	+0.15	P(14)	4199.99	4199.93	+0.06
R(14)	4308.94	4308.98	-0.04	P(15)	4195.25	4195.12	+0.13
R(15)	4311.55	4311.69	-0.14	P(16)	4190.40	4190.25	+0.15
R(16)	4314.32	4314.34	-0.02	P(17)	4185.39	4185.30	+0.09
R(17)	4316.87	4316.92	-0.05	P(18)	4180.36	4180.29	+0.07
R(18)	4319.50	4319.43	+0.07				
R(19)	4321.83	4321.86	-0.03				
R(20)	4324.13	4324.23	-0.10				
R(21)	4326.56	4326.53	+0.03				
R(22)	4329.75	4329.76	-0.01				

TABLE IV. Molecular constants of C¹²O¹⁶ and C¹³O¹⁶.

	Fundamental	C ¹² O ¹⁶ Overtone	C ¹² O ¹⁶ Herzberg ¹	C ¹³ O ¹⁶ Fundamental
$\nu(0-1)$	2143.16 cm ⁻¹			2096.05 cm ⁻¹ (obs.)
$\nu(0-2)$		4259.88 cm ⁻¹		
ω_e	2169.60 cm ⁻¹		2168.2 cm ⁻¹	2121.33 cm ⁻¹ (calc.) [*] 2121.24 cm ⁻¹ (calc.) ^{**}
$x_e\omega_e$	13.22 cm ⁻¹			12.64 cm ⁻¹ (calc.) ^{***}
α	0.0175 cm ⁻¹	0.0174 cm ⁻¹	0.01744 cm ⁻¹	0.0169 cm ⁻¹ (obs.) 0.0168 cm ⁻¹ (calc.) ^{****}
$B''(v=0)$	1.9150 cm ⁻¹	1.9150 cm ⁻¹		1.8380 cm ⁻¹ (obs.)
$B'(v=1)$	1.8975 cm ⁻¹			1.8211 cm ⁻¹ (obs.)
$B'(v=2)$		1.8802 cm ⁻¹		
B_e	1.9238 cm ⁻¹		1.9310 cm ⁻¹	1.8465 cm ⁻¹
I_e	14.548 × 10 ⁻⁴⁰ g cm ²			15.157 × 10 ⁻⁴⁰ g cm ²
r_e	1.1303 Å		1.1284 Å	1.1280 Å
k_{111}	-62.78 cm ⁻¹			-60.70 cm ⁻¹
k_{1111}	13.35 cm ⁻¹			12.77 cm ⁻¹

^{*} Calculated from Eq. (2) using $\nu(0-1)'$ and $(x_e\omega_e)'$.

^{**} Calculated from Eq. (12).

^{***} From Eq. (13) using B_e' , ω_e' , and k_{111}' , or Eq. (15).

^{****} From Eq. (12) using k_{111}' , k_{1111}' , and ω_e' .

¹ G. Herzberg, *Molecular Spectra and Molecular Structure*, Part I, "Diatomic Molecules" (Prentice Hall, Inc., New York, 1939), p. 486.

between the frequencies and the k 's:

$$\begin{aligned} (\omega_e'/\omega_e) &= (\mu/\mu')^{\frac{1}{2}}, \\ k_{111}' &= k_{111}(\omega_e'/\omega_e)^{\frac{3}{2}}, \\ k_{1111}' &= k_{1111}(\omega_e'/\omega_e)^2, \end{aligned} \quad (12)$$

where the prime refers to the isotopic molecule.

In the solution of the quantum-mechanical

problem to second order of approximations for the energy,³ it is found that the constants $x_e\omega_e$ and α in (1) may be expressed in terms of the constants k_{111} and k_{1111} as follows:

$$x_e\omega_e = \frac{1}{4}[6k_{1111} - 15(k_{111}^2/\omega_e)], \quad (13)$$

$$\alpha = -6(B_e/\omega_e)[B_e + 2k_{111}(2B_e/\omega_e)^{\frac{1}{2}}]. \quad (14)$$

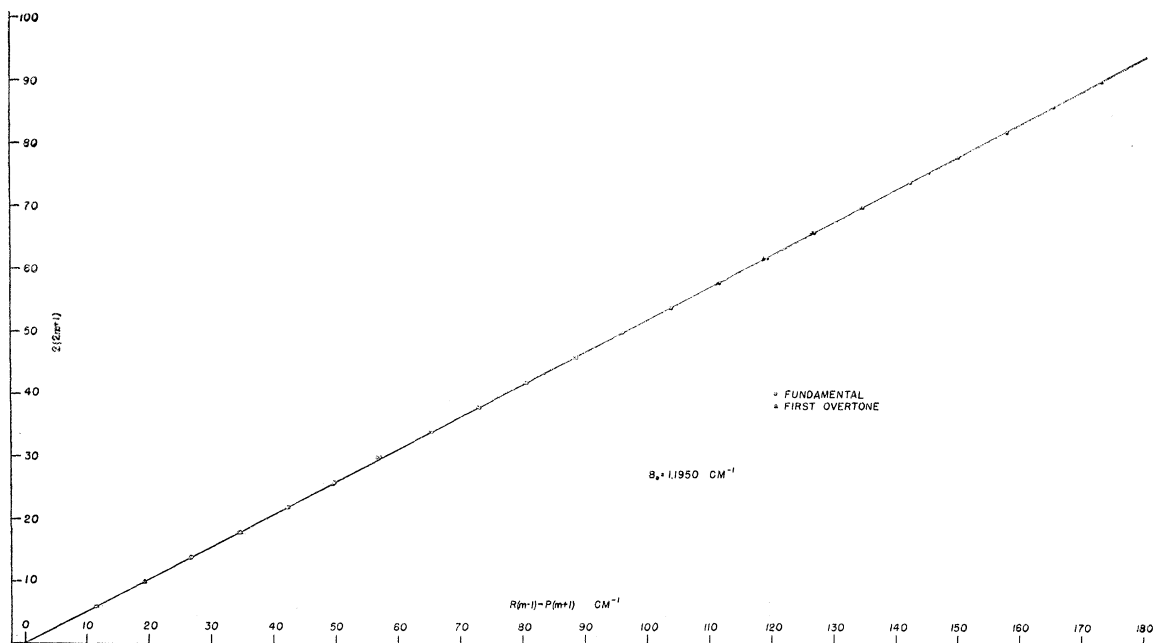


FIG. 3. Plots of $R(m-1) - P(m+1)$ versus $2(2m+1)$ for fundamental and first overtone vibration-rotation bands of C¹²O¹⁶.

³ A. H. Nielsen, *J. Chem. Phys.* **11**, 160 (1943), see x_{11} and α_1 of Eq. (15).

By substituting the experimental values of $x_e\omega_e$, ω_e , B_e , and α into (13) and (14), k_{111} and k_{1111} were found and are given in Table IV. The corresponding k_{111}' and k_{1111}' were then found from Eqs. (12) and are also listed in Table IV. By substituting the values of k_{111}' , B_e' , ω_e into (14), the value of α' was found to be 0.0168 cm^{-1} as compared with the experimental value of 0.0169 cm^{-1} . $(x_e\omega_e)'$ found in Table IV was

computed by substituting k_{111}' and k_{1111}' and ω_e' into Eq. (13). This is equivalent to the relation

$$(x_e\omega_e)'/(x_e\omega_e) = (\omega_e'/\omega_e)^2. \quad (15)$$

The equilibrium value ω_e' was computed from the ratio of the reduced masses and ω_e , Eq. (12). All the constants computed have been tabulated in Table IV.

Negative Corona in Freon-Air Mixtures

G. L. WEISSLER AND E. I. MOHR

Department of Physics, University of Southern California, Los Angeles, California

(Received April 7, 1947)

In order to gain information as to the importance of negative space charges in coronas, studies of negative corona in freon-air mixtures were undertaken. The mixtures used ranged from 10^{-4} to 10^2 percent of freon-12 in dry air. The onset potentials of the intermittent corona region were constant in all mixtures, approximately 6 to 7 kv with X/p about 100; only in pure freon it changed to 12,600 volts with X/p about 200. Concentrations of freon up to one percent revealed corona characteristics very similar to those of air. From one to 20 percent mixtures showed rapidly decaying Trichel pulses. Upon analysis this seems due to the formation of Cl^- and F^- , which are

shown to be still stable at values of $X/p \geq 200$. As a consequence, negative space charges will be stable in regions much closer to the corona point than in air and will, therefore, be more efficient in suppressing the discharge as is indicated by decaying pulse sizes. At still higher concentrations the more stable Cl^- and F^- formed heavier space charges, inhibiting the formation of large electron avalanches to such an extent that only incipient Trichel bursts were produced. Thus the range of potential of the intermittent corona region was extended to higher values, and the corona current *vs.* potential curves showed rapidly decreasing slopes with increasing amounts of freon.

INTRODUCTION

THIS investigation was undertaken for two reasons: to explain in more detail the mechanism that is active in the suppression of sparks because of the presence of gases which form very stable negative ions; and to investigate the character of space-charge pulses in such coronas in order to further our understanding of the more general mechanisms active in spark breakdown in any gas. It is essential to state the reasons for utilizing corona studies for this purpose rather than studies of sparking potentials with plane parallel electrodes. The propagation of a discharge at or near atmospheric pressure is mainly based on the formation of streamers proceeding from the anode or the mid-gap region. This occurs only near a threshold value. A plane parallel gap does not lend itself easily to a detailed study of the mechanisms involved because of the rapidity of events succeeding the

initiating streamer. In a corona, however, the range of potentials from onset to spark breakdown is wide. In addition, there are the inherent advantages of strongly divergent electric fields and differences in mechanisms between positive and negative coronas. The proper choice of the geometry of corona gaps, i.e., confocal paraboloids or a hyperboloid point electrode opposite a plane enables one to make field calculations and to observe space-charge phenomena which are obscured in experiments on plane parallel gaps.

The characteristic curves of any point-to-plane corona, plotting the gap current against the applied potential, are made up of three ranges of specific interest. The "dark-current" range occurs well below the onset of any visible corona, and the sharper the point the narrower this range will be. It depends most strongly on the first Townsend coefficient α and to a lesser degree